Multiscale recursion in dense hydrogen plasmas

Stéphane Bagnier,* Pierre Dallot, and Gilles Zérah
Commissariat à l'Energie Atomique, BP 12, 91680 Bruyères-le-Châtel, France
(Received 24 September 1999)

We present and assess a multiscale recursion method to calculate electronic density via the Green's function. The method lies within the framework of finite temperature density functional theory and uses a real space approach. It provides a satisfactory description of the first Brillouin zone without invoking k points. Unlike methods that explicitly calculate eigenstates, the computational workload decreases with temperature. Tests are performed on a system representing a hydrogen plasma with a local pseudopotential. Calculations are distributed on real space grids with different spacings using scaling properties of the recursion. The computational workload increases linearly with the size of the system and can be productively dispatched on an arbitrarily large number of processors.

PACS number(s): 52.65.−y, 71.15.Mb, 71.23.An

I. INTRODUCTION

Interest in dense hydrogen plasmas is threefold. First, these plasmas are important in astrophysics [1] since hydrogen is responsible for 80% of our solar system. Second, they are the core of inertial confinement fusion. Their description is thus a technological issue. Last, a plasma phase transition might occur at temperatures and densities characteristic of giant planets and low-mass brown dwarfs [2,3]. The plasma properties relevant to these problems (equation of state, conductivity, viscosity) depend on modeling the electronic screening of the field created by the ions. This problem has recently been tackled using a variety of methods (see [4] for a comparison). Path integral Monte Carlo calculations have been performed to investigate the existence of a plasma phase transition [5]. Other methods rely on a more approximate treatment of the interacting many-fermion problem, using either the tight binding model [6] or the local density approximation of the density functional theory (DFT/LDA). Clerouin and co-workers performed *ab initio* molecular dynamics using Thomas-Fermi-like functionals [7,8,4]. The dynamical variable is then the electronic density directly and no electronic state needs to be considered. This method, however, has the shortcomings of the Thomas-Fermi approximation. An important step toward an accurate simulation of plasmas was taken by Alavi and co-workers [9–13]. The electronic density is obtained by summing up the squares of occupied wave functions. Because the number of occupied states increases rapidly with temperature, their method is usually limited to temperatures smaller than a few eV.

A method to calculate the electronic density with the same accuracy without recourse to eigenstates would thus be quite useful. This is the main thrust of our work. In this paper, we present a method to calculate accurate electronic densities at higher temperatures from a local pseudopotential. The case of hydrogen is simple in this respect because core electrons are irrelevant. The pseudopotential aims at representing smoothly the Coulomb singularity in a sufficiently large energy range [15].

The method we present is a finite temperature extension of the proposal of Baroni and Giannozzi [16]. Considering a silicon crystal at zero temperature, they performed a recursion on a regular grid in real space using a finite difference representation of the Hamiltonian to compute the diagonal term of the Green's function. The computation time is then proportional to the number of atoms in the cell (order N method), in contrast to the square of this number for schemes involving eigenstates. The prefactor, however, was very large and the method was not competitive with diagonalization techniques. A finite temperature extension of the recursion method has already been introduced in the context of bond order potentials [17,18], essentially as an artificial way to broaden the Fermi surface. Because of the subsequent damping of Friedel's oscillations, the convergence of the recursion is substantially improved. Thus, it seems natural to investigate the behavior of a real space recursion scheme when the electronic temperature is finite, as is the case in a plasma. The resulting method can be expected to provide order N parallelized code, whose computational speed increases with temperature, because of enhanced localization of the density matrix [19]. This is, of course, in sharp contrast to wave function methods.

We first give a brief overview of the Green's function and recursion techniques that we use and of their application to the calculation of the electronic density in a hydrogen plasma. We then present several approximations that we explain from a local density of states (LDOS) viewpoint, and compare the results with those of the free energy functional molecular dynamics (FEMD) code of Alavi *et al.* [12,14]. We finally propose and assess a multiscale recursion method.

II. GENERAL BACKGROUND

Following [12], we place ourselves within the finite temperature DFT framework [20,21]. We use Mermin's functional together with the Kohn and Sham approximation to the kinetic energy. The local density approximation is used to describe exchange and correlation. Thus, the electronic density is the weighted sum of the squares of one-electron eigenfunctions:

*Author to whom correspondence should be addressed. Electronic address: bagnier@bruyeres.cea.fr

$$\rho(r)=\sum_i f_i\phi_i^*(r)\phi_i(r). \tag{1}$$

In this expression, the factor f_i is the Fermi-Dirac occupation $f_i=(1+e^{\beta(\epsilon_i-\mu)})^{-1}$, the chemical potential μ is chosen to achieve electric neutrality, and the one-electron eigenfunctions are the self-consistent solutions that minimize Mermin's functional. They are solutions of

$$\left(-\frac{\Delta}{2}+v_{\rm eff}(r_i)\right)\phi_i(r_i)=\epsilon_i\phi_i(r_i). \tag{2}$$

When the interaction with the ions is represented by a pseudopotential $v_{\rm ps}$, the self-consistent effective potential $v_{\rm eff}$ is obtained from the electronic density and the ionic positions as

$$v_{\rm eff}(r)=\int\frac{\rho(r')}{|-r'|}dr'+\sum_{\rm ions}v_{\rm ps}(|r-R_i|)+v_{\rm xc}(\rho(r)). \tag{3}$$

Hence, the electronic density determines the potential, but the density depends on the potential by means of the one-electron wave functions. Our objective is to bypass the calculation of wave functions when calculating the density from the potential. This is possible using Green's function techniques combined with the recursion method. The electronic density can be directly expressed in terms of the one-electron Green's function:

$$\rho(r)=-\frac{i}{\pi}\oint f(z)G(r,z)dz. \tag{4}$$

In this expression, the integral is performed on a contour in the complex energy plane which contains the relevant poles of the Hamiltonian but leaves out the poles of $f(z)$. The factor $G(r,z)$ is the diagonal element of the Green's operator calculated at a real space point r:

$$G(r,z)=\langle r|\hat{G}(z)|r\rangle=\langle r|(z-\hat{H})^{-1}|r\rangle. \tag{5}$$

The recursion method permits an efficient calculation of the diagonal matrix elements of the Green's function in any state [22,23]. Expression (5) assumes the use of the localized basis $|r\rangle$. Expressing the Hamiltonian in this basis is therefore a prerequisite to performing the recursion. This can be done by means of a finite difference approximation, as shown in Ref. [16]. Given an appropriate formulation for the Hamiltonian, the recursion is performed by constructing a chain of states. The initial state is $|u_0\rangle=|r\rangle$. The principle is then to describe how this localized state is coupled by the Hamiltonian to its environment. A part of $\hat{H}|u_0\rangle$ projects onto $|u_0\rangle$. The rest of it is orthogonal to $|u_0\rangle$ and defines a new state $|u_1\rangle$:

$$\hat{H}|u_0\rangle=\alpha_0|u_0\rangle+b_1|u_1\rangle. \tag{6}$$

The normalized state $|u_1\rangle$ is then coupled by the Hamiltonian to a new state, orthogonal to both $|u_0\rangle$ and $|u_1\rangle$. The recursion is the iteration of this process, which defines sequences of states and recursion coefficients. Further in the chain, a recursion state $|u_n\rangle$ is coupled to the states that are immediately before and after it:

$$\hat{H}|u_n\rangle=b_n|u_{n-1}\rangle+a_n|u_n\rangle+b_{n+1}|u_{n+1}\rangle. \tag{7}$$

This equation defines $|u_{n+1}\rangle$, b_{n+1}, and a_n. The recursion coefficients are

$$a_n=\langle u_n|\hat{H}u_n\rangle,\quad b_n=\langle u_{n-1}|\hat{H}|u_n\rangle. \tag{8}$$

These coefficients are, respectively, the energy in the state $|u_n\rangle$ and the hopping integral between states $|u_{n-1}\rangle$ and $|u_n\rangle$. In summary, the recursion produces an orthogonal basis of states in which the Hamiltonian has a tridiagonal form. This remarkable property allows the diagonal element of the Green's function $G(r,z)=\langle u_0|\hat{G}(z)|u_0\rangle$ to be written as a continued fraction in terms of the recursion coefficients a_n and b_n [24]:

$$G(r,z)=\cfrac{1}{z-a_0-\cfrac{(b_1)^2}{z-a_1-\cfrac{(b_2)^2}{z-a_2-\cdots}}}. \tag{9}$$

The local density of states can then be computed as

$$n(E,r)=-\frac{1}{\pi}\lim_{s\to 0^+}\mathrm{Im}\,G(r,E+is). \tag{10}$$

To simplify notations, we will denote the LDOS by $n(E)$, the real space location being always implicit. As the knowledge of the LDOS leads to the electronic density in r, the recursion coefficients together with Eq. (1) are sufficient. As will be shown, the recursion coefficients that we generate fluctuate around some constant values, and converge to these values when the rank increases. We will therefore use linear response around the constant chain model, which can be found in Ref. [23].

The constant chain model is obtained when the coefficients a_n and b_n are constants equal to a and b. Haydock shows that the local density of states associated with this chain forms an arc with center a and width $2b$:

$$n(E)=\begin{cases}\sqrt{4b^2-(E-a)^2}/4b^{1/2} & \text{if } a-2b\leqslant E\leqslant a+2b\\ 0 & \text{otherwise.}\end{cases} \tag{11}$$

Assuming $a=2b$, the lower band edge is equal to zero. Remark that $n(E)$ has been normalized so as to be independent of $a=2b$ in the limit of small energies. Fluctuations δa_n and δb_n around the constant values a and b generate modifications in the LDOS. Within linear response, Haydock shows that the correction $\delta n(E)$ to the above density is equal to

$$\delta n(E)=\frac{1}{\pi^2 b^{1/2}}\sum_{n=0}^{\infty}\{\delta a_n\sin[(2n+2)\theta]+\delta b_{n+1}\sin[(2n+3)\theta]\}, \tag{12}$$

where θ is a reduced variable ranging from zero to π:

$$\theta = \cos^{-1}\left(\frac{E-a}{2b}\right). \quad (13)$$

The δa_n and δb_n induce corrections in the LDOS which are, respectively, antisymmetric and symmetric with respect to the center of the distribution. The fluctuations associated with very large values of n do not strongly affect integrated quantities such as the electronic density, thus justifying an approximate treatment of the continued fraction [Eq. (9)] for large n. As will be seen, our calculated coefficients always saturate around some constant values. This will allow the use of the constant chain terminator suggested by Haydock: we will replace the exact coefficients with the constant values after a certain rank.

III. REFERENCE SYSTEM

Throughout this work, we compare our results with those obtained from a different method to calculate the electronic density. This reference method is that used in the free energy functional molecular dynamics code of Alavi and co-workers [12,14]. It consists of diagonalizing the operator $e^{-\epsilon\hat{H}}$ using the Lanczos algorithm [25]. This operator has the same eigenvectors as the Hamiltonian. When ϵ is small, it is easier to diagonalize than the Hamiltonian, because it is better conditioned.

The electronic density is then calculated as the sum of the squares of the eigenvectors. This technique is performed on a system contained in a periodic box. Hence, the eigenvectors of the Hamiltonian are Bloch functions $\psi_{nk}(r) = u_{nk}(r)\exp(i\mathbf{k}\cdot\mathbf{r})$, where u_{nk} has the same periodicity as the potential, and where k belongs to the first Brillouin zone. Following [26–28], the summation upon the first Brillouin zone, required, for example, when calculating the electronic density, is usually reduced to a finite sum over a small number of special k points. The number of k points retained in the calculation then determines the accuracy of the calculation. The most drastic approximation consists of retaining only the center of the first Brillouin zone: the Γ point. In this case, the calculated wave functions have the same periodicity as the potential. This approximation may have severe consequences, especially when the simulation box is small. Alavi emphasized that the Γ point restriction could skew quantitative calculations for hot dense hydrogen [13]. Recently, Deutsch implemented a many-k-point ability into the FEMD code [14]. In this article, we will first use the Γ-point restriction for testing the recursion method and evaluating the accuracy of the real space discretized kinetic operators. Then we will go beyond this approximation, and compare our results with eight-k-point FEMD calculations.

The physical system upon which the comparisons will be made is a hydrogen plasma. The plasma is simulated within a cubic box with periodic conditions in the three directions of space. The electron-ion interaction potential is represented by a local pseudopotential which smooths out the Coulomb singularity in the vicinity of the ions. The pseudopotential that we use has been proposed by Giannozzi [15]:

$$v_I(r) = -\frac{1}{r}\mathrm{erf}\left(\frac{r}{r_{c1}}\right) + (a+br^2)\exp\left[-\left(\frac{r}{r_{c2}}\right)^2\right], \quad (14)$$

TABLE I. Characteristics of the test system.

Temperature	3 eV
Density	0.5 g/cm^3
Ion sphere radius	$r_s = 1.72$ a.u.
Coupling parameter	$\Gamma = E_{\mathrm{Coulomb}}/E_{\mathrm{kinetic}} \approx 5.2$
Degeneracy	$\theta = T/T_{\mathrm{Fermi}} \approx 0.18$
Side of the simulation cell	7 a.u.
Composition	16 hydrogen atoms
Discretization	32 points per dimension
Energy cutoff	103 a.u.
Boundary conditions	periodic

where $r_{c1} = 0.25$, $a = -1.9287$, $b = 0.3374$, and $r_{c2} = 0.284$ (all in a.u.).

The value of this pseudopotential at the origin is equal to a, which is about -2 hartree≈ -55 eV. Hence, we expect this potential to give a reasonable description of the density up to temperatures of 5 eV.

The location of the atoms was obtained from a short run of molecular dynamics performed with the FEMD code. The initial configuration was bcc, but the temperature (3 eV) was sufficient to obtain disordered configurations. The simulation was stopped when the averaged atomic motion was larger than the interatomic distance. The degree of disorder was then considered to be sufficient. The characteristics of the test system are listed in Table I.

This reference ionic configuration was then used to calculate self-consistent electronic densities using respectively one and eight k points. The electronic density was converged with respect to the number of k points in the second case. In both cases, the electronic density ρ_A (see Fig. 3 below) and the self-consistent electronic and chemical potentials u_{eff} and μ were stored. The potentials are to be used as input parameters in our recursion calculations. The resulting density ρ_R is then to be compared with the relevant reference density ρ_A.

IV. TESTS OF THE RECURSION METHOD

As a first step toward constructing an efficient algorithm, we present a first implementation of the recursion technique that serves as a test of our recursion procedure. This simple case will be used later to assess further approximations. We restrict ourselves to the Γ point, that is, we consider only periodic states. This approach allows the use of the fast Fourier transform (FFT) to compute $\hat{H}|u_n\rangle$.

A. Continuous Fourier recursion method

The kinetic term of $\hat{H}$ is diagonal in Fourier space, with eigenvalues $k^2/2$. When using the FFT to compute this term, the only approximation performed is the grid cutoff. We denote this method ''continuous,'' as opposed to the real space discretized methods that we examine in the next section. We start the recursion with a state localized in one of the grid cells in the simulation box: $|u_0\rangle = |r\rangle$. Let $|u_n\rangle$ be the nth state in the chain; the next state is obtained by applying the following procedure.

(1) Apply $\hat{H}$ onto $|u_n\rangle$. The Fourier transform of $|u_n\rangle$ is

$$|v\rangle \leftarrow \mathcal{F}[|u_n\rangle].$$

Next, we apply the kinetic energy operator (diagonal in reciprocal space),

$$|v\rangle \leftarrow |v\rangle \frac{k^2}{2}.$$

We transform back $|v\rangle$ in real space,

$$|v\rangle \leftarrow \mathcal{F}^{-1}[|v\rangle].$$

Then we add the potential energy,

$$|v\rangle \leftarrow |v\rangle + v_{\text{eff}}|u_n\rangle.$$

(2) Calculate a_n.

$$a_n = \langle u_n|\hat{H}|u_n\rangle = \langle u_n|v\rangle.$$

(3) Prepare the next chain state $|u_{n+1}\rangle$.

$$|u_{n+1}\rangle \leftarrow (\hat{H} - a_n)|u_n\rangle - b_n|u_{n-1}\rangle = |v\rangle - a_n|u_n\rangle - b_n|u_{n-1}\rangle.$$

(4) Calculate b_{n+1}.

$$b_{n+1}^2 = \langle u_{n+1}|u_{n+1}\rangle.$$

(5) Normalize $|u_{n+1}\rangle$.

$$|u_{n+1}\rangle \leftarrow \frac{1}{b_{n+1}}|_{n+1}\rangle.$$

Note that the first step in the chain is singular, because the state $|u_{-1}$ does not exist. The coefficient b_0 is taken equal to zero.

We first test the method in the case of a free electron in a periodic box. The simulation box is the one described in the preceding section, but the electronic potential is set equal to zero. The initial state is localized into one of the elementary cells constituting the grid. This elementary cell is a cube with a side h equal to the grid spacing (the 32nd part of the side of the simulation box). Because of periodic conditions, this elementary state is reproduced in every image of the simulation box: the electronic state has the simulation box periodicity.

The recursion coefficients obtained are plotted in Fig. 1. They fluctuate around some constant values, and the fluctuations of a_n and b_n seem correlated to one another. Note that these coefficients are very different from those calculated by Haydock in the case of a free electron placed in an infinite space [23]. The first are approximately constant, whereas the second tend to infinity as n increases. This difference can be understood from the LDOS. The fact that the simulation box is discretized in real space implies the existence of a cutoff in k space: kinetic energies larger than $3(2\pi/h)^2/2$ cannot be reached (see Fig. 2). Hence, the LDOS of our discretized system forms an isolated band which can be described, to a first approximation, by the constant chain model. In our case, the constants are $a \approx 140$ and $b \approx 70$. These are respectively one-half and one-quarter of the bandwidth of the constant chain LDOS, as can be checked on Fig. 2. The fluctuations δa_n and δb_n have the effect of correcting the shape of the

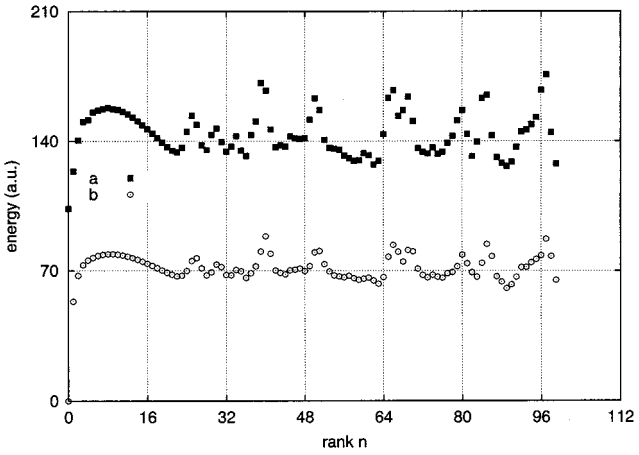

FIG. 1. Calculated coefficients a_n and b_n obtained using the continuous Fourier recursion method in the free electron case.

LDOS according to formula (12). Hence, the observed saturation of the chain coefficients is directly related to the use of a grid to represent the electrons. Because this feature is shared by all the models that we will consider, it will always be possible to use the constant chain terminator (see Sec. II).

We now turn to the calculation of the electronic density ρ_R in the model system of Sec. III. A recursion of 100 steps was initiated in each grid cell. The recursion coefficients were calculated in this process. The Green's function could then be obtained as a continued fraction using the recursion coefficients and the constant chain terminator (the constants used were the last values of a_n and b_n calculated). The electronic density is finally calculated by performing a contour integral in the complex energy plane according to Eq. (1).

In this case the recursion scheme assumes periodic conditions for the chain states. Hence, the recursion describes only periodic states. The FEMD calculation that we must compare to is therefore the one performed using only the Γ point. The two methods then solve the very same problem, and, indeed,

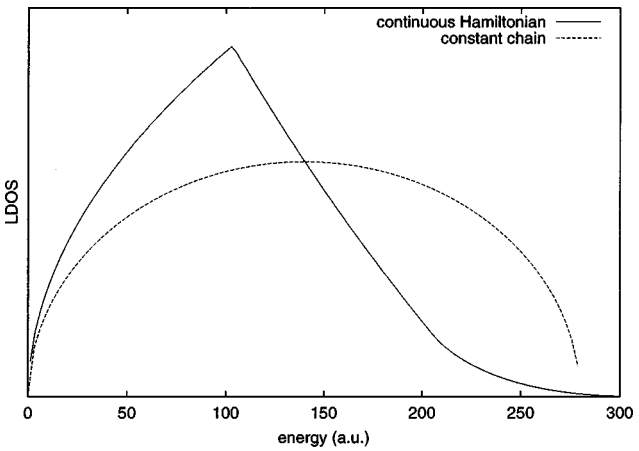

FIG. 2. Free electron case: LDOS in the periodic box and LDOS of the related constant chain model. The lower bound is equal to zero and the upper bound is dictated by h, the step of the discretization. $E_{\max} = k_{\max}^2/2 = 3\pi^2/2h^2 \approx 310$ a.u. By comparison, the cutoff energy used in the FEMD calculation is about $E_{\text{CUT}} = k_{\text{CUT}}^2/2 = \pi^2/2h^2 \approx 103$ a.u.

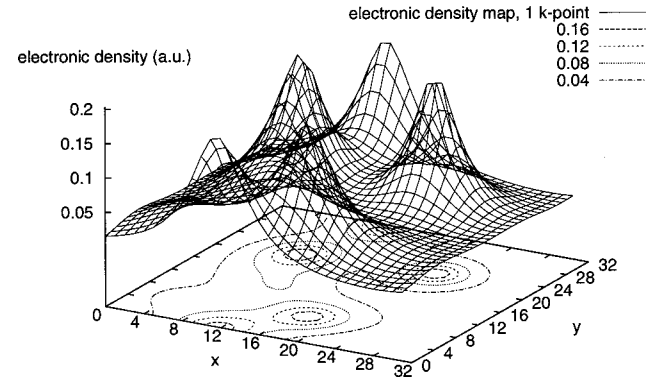

FIG. 3. Reference electronic density ρ_A on a section of the system. The zones of high density correspond to ion locations. The density is approximately constant in between.

the density ρ_R is then essentially similar to ρ_A (Fig. 3). The map of differences is shown in Fig. 4.

The density ρ_R is thus very close to ρ_A. It is slightly larger, showing a maximum difference of 2% localized close to the ions. We attribute this positive difference to the fact that the two methods do not share the same kinetic operator approximations. Then the calculated density ρ_R cannot be strictly consistent with the effective and chemical potentiels. We expect that a self-consistent calculation could diminish the overscreening seen in Fig. 4. This result validates the recursion procedure, the use of a constant terminator, and the calculation of the density [Eqs. (1) and (4)].

B. Real space discretized kinetic operator

Between 1992 and 1997, Baroni and Giannozzi and Gebauer performed recursions using a kinetic operator discretized in real space. They used three- [16] and five-point [29] finite difference formulas. The discretized Hamiltonian can be expressed in Fourier space or directly used in real space, with no recourse to Fourier transforms.

Let h be the grid spacing, and $\langle r_j|\hat{H}|r_i\rangle$ the coupling between a state localized in r_i and a state localized in r_j. The three-point formulas are

$$\langle r_j|\hat{H}|r_i\rangle=\begin{cases} 3/h^2+v_{\text{eff}}(r_i) & \text{if } r_i=r_j \\ -1/2h^2 & \text{if } |r_i-r_j|=h \\ 0 & \text{otherwise.} \end{cases} \tag{15}$$

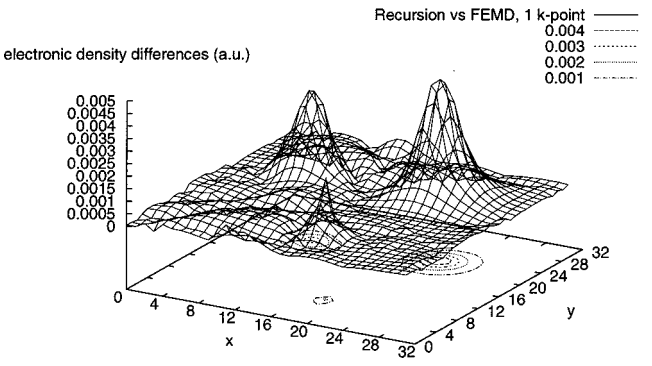

FIG. 4. $|\rho_R-\rho_A|$: density differences between the two methods, related to the section shown in Fig. 3.

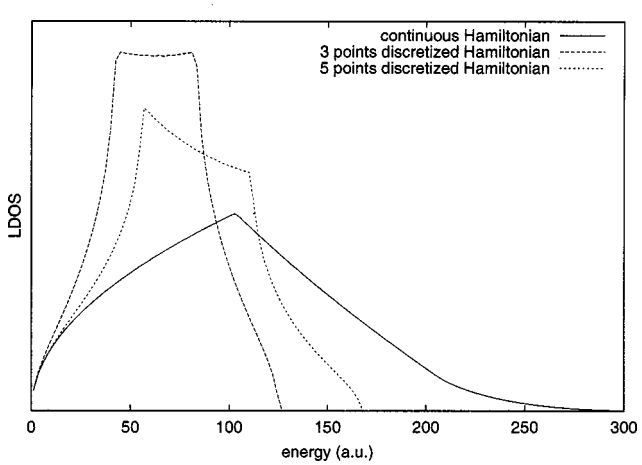

FIG. 5. Density of states related to the continuous and discretized Hamiltonians (three and five points).

Expressed in Fourier space, this kinetic operator is diagonal and its eigenvalues are

$$E_K(k_x,k_y,k_z)=-\frac{\cos(k_xh)+\cos(k_yh)+\cos(k_zh)-3}{h^2}. \tag{16}$$

If we use five points instead of three, the formulas are

$$\langle r_j|\hat{H}|r_i\rangle=\begin{cases} 90/(24h^2)+v_{\text{eff}}(r_i) & \text{if } r_i=r_j \\ -16/(24h^2) & \text{if} |r_i-r_j|=h \\ 1/(24h^2) & \text{if} |r_i-r_j|=2h \\ 0 & \text{otherwise} \end{cases} \tag{17}$$

and in reciprocal space

$$E_K(k_x,k_y,k_z)=\frac{1}{6h^2}\left(16\sum_i^{xyz}\cos(k_ih)-\sum_i^{xyz}\cos(2k_ih)-15\right). \tag{18}$$

Again, we first consider the free electron case in a periodic box. The eigenvalues of the discretized Hamiltonians tend to those of the continuous Hamiltonian when $|k|$ is small. For larger values of $|k|$, the change in the eigenvalues can be interpreted as a change in the LDOS which is represented in Fig. 5. On this figure, we clearly see that the five-point formula is more accurate than the three-point one, because the associated density of states is closer to the exact one in a larger energy zone.

The recursion coefficients for a free electron in a periodic box related to the five-point discretized Hamiltonians are shown in Fig. 6 and listed in Table II. The coefficients show saturations for smaller values than they did with a continuous Hamiltonian, because the bandwidths associated with the discretized Hamiltonian are smaller (see Fig. 5). The fluctuations around these constant values are also much smaller. Moreover, the value of a_n calculated with the three-point formula is exactly constant. This is because fluctuations in a_n would generate antisymmetrical corrections to the constant chain LDOS (Fig. 2), whereas the three-point LDOS is ex-

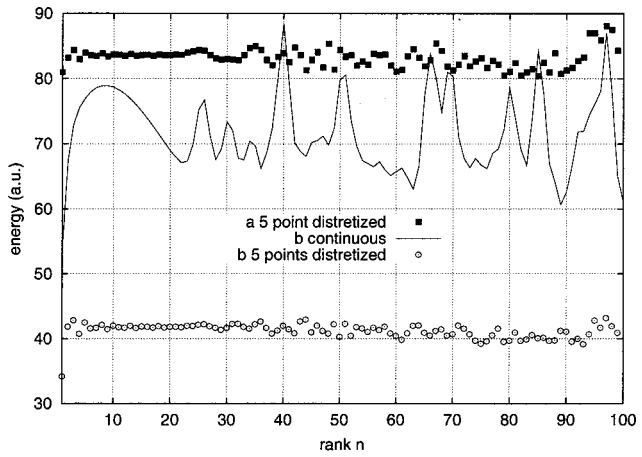

FIG. 6. Recursion coefficients a_n and b_n for a free electron in a periodic box, calculated (1) with a continuous Hamiltonian (solid line) and (2) with a five-point formula within the conditions of Fig. 1 (dots).

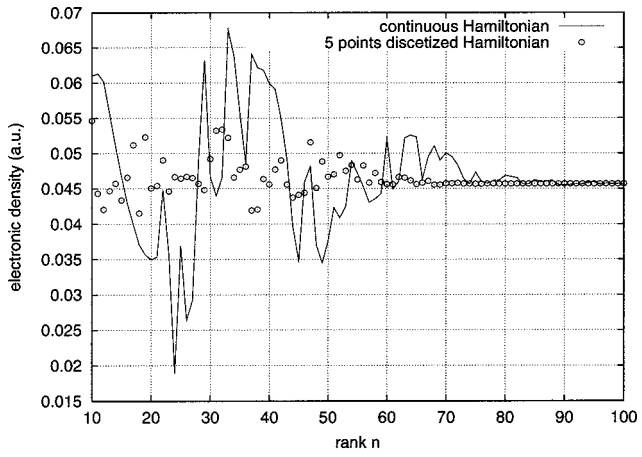

FIG. 7. Convergence of the electronic density as a function of the number of recursion coefficients taken into account. The five-point scheme converges faster.

actly symmetrical with respect to the center of the band (Fig. 5). Fluctuations in a_n are therefore unnecessary to obtain the exact three-point LDOS.

We next compare the convergence properties of various schemes in the free electron case. A temperature of 3 eV is assumed. The chemical potential is evaluated within the Thomas-Fermi approximation, assuming a density corresponding to 16 electrons in the simulation cell. This approximation should not affect the convergence rate. We then calculate the density as a function of the number n of recursion coefficients taken into account (we replace the coefficients of rank higher than n by a_n and b_n). The results are shown in Fig. 7.

The densities converge toward the same limit despite the fact that the densities of states are very different. This is because the occupied states have small energies (compared to a, for instance), and because the various expressions for the kinetic energy are equivalent in this limit. The faster convergence of the discretized schemes is interpreted as follows: The densities of states related to discretized schemes are closer to their associated constant chain densities of states. Hence, small corrections $\delta n(E)$ to the constant chain model are sufficient to obtain an accurate representation of the exact LDOS and, therefore, of integrated quantities such as the electronic density.

We now compare the discretized schemes with the reference method (see Fig. 8). The FEMD code yields a potential v_{eff} a chemical potential μ, and an electronic density ρ_A calculated with the Γ point only. Using the potentials, we calculate an electronic density ρ_R from the recursion method and the discretized schemes. The three-point scheme is found to yield correct results almost everywhere, except in the vicinity of the ions, where we find up to 6% difference with respect to ρ_A. The three-point approximation introduces a systematic error, which can only be avoided by using a finer grid and so increasing the computation time. By contrast, the density differences obtained between the five-point scheme and (1) the continous Hamiltonian, and (2) the reference FEMD calculation ρ_A (both in Sec. IV A), are both smaller than 2%. It is concluded that the five-point discretization does not alter the precision of the recursion scheme in these conditions. We therefore retain the five-point scheme in the rest of this work.

At this point, we have implemented the recursion method and validated the use of a constant terminator. We have also found an approximation to the continuous Hamiltonian which is accurate and can be used without recourse to k space. Thus, the recursion can now be implemented in real space and it need not be constrained by the limits of the simulation cell. The cell itself is extended by periodicity, but the chain states need no longer be subject to periodic conditions. The recursion scheme is then equivalent to using many k points in a FEMD calculation. However, extending the chains is computationally expensive since computation time grows like the fourth power of the chain length. We now present a strategy that allows extending the chains at a reasonable cost.

V. MULTISCALE STRATEGY

When concluding their paper [16], Baroni and Giannozzi remarked that recursion chains starting from neighboring

TABLE II. Recursion coefficients for a free electron. Units are a.u. throughout.

	Continuous Hamiltonian	Five-point discretized Hamiltonian	Three-point discretized Hamiltonian
Average value of a	≈140	≈80	≈60
Average value of b	≈70	≈40	≈30
Fluctuations in a	≈20	≈5	no fluctuation
Fluctuations in b	≈10	≈2	≈2

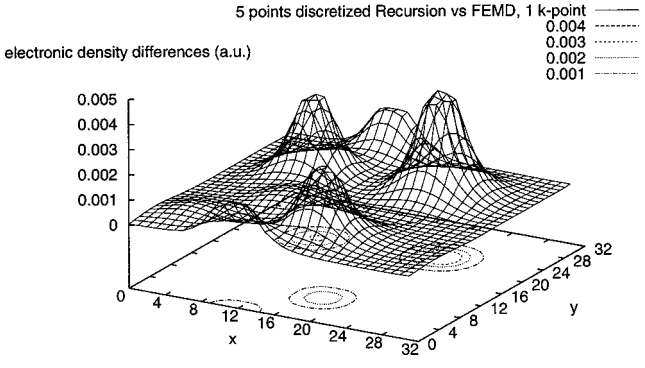

FIG. 8. $|\rho_R-\rho_A|$: absolute differences in the calculated densities between the reference model (Γ point) and the recursion performed in the five-point scheme. The differences are calculated on the section of the simulation box shown in Fig. 3.

points contain almost the same information. Hence, much of the calculation performed in the recursions appears to be redundant. In their conclusion, they envisioned the use of a hierarchy of chains related to different grid spacings, which would allow the calculation of better terminators. Unfortunately, this procedure was never implemented. We now propose an analysis of the recursion coefficients that permits a practical use of this idea.

As seen in Sec. II, the recursion coefficients are aliases of the LDOS. Within linear response theory, the recursion coefficients can be calculated from the LDOS as the coefficients that dictate its shape in a certain basis [Eq. (12)]. Hence, the coefficients vary continuously from one cell to another, because the LDOS does. In addition, the recursion coefficients represent couplings between consecutive chain states. The chain states generated in our recursions take significant values within zones that can be schematically represented as spheres with radii proportional to the rank in the chain. The nth recursion coefficients thus represent the response at the center of the sphere to perturbations in the zone described by the sphere, as mediated by the chain states of order lower than n. The recursion coefficients related to two neighboring cells will therefore be closer when the rank is large, because the spheres tend to be identical. This trend is observed in the calculated coefficients (see Fig. 9).

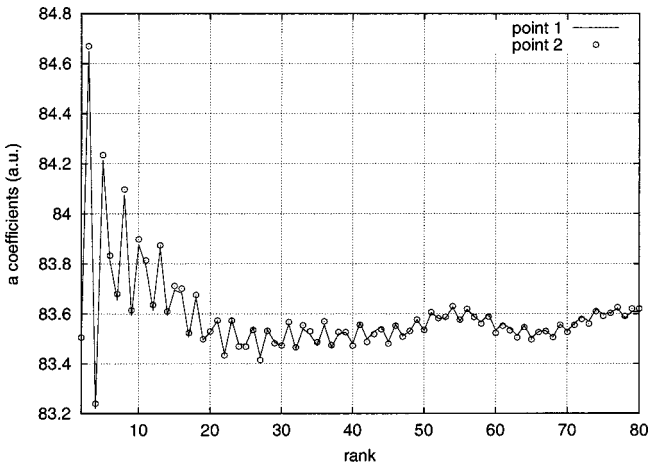

FIG. 9. Coefficients a_n related to two neighboring points 1 and 2 in the model system.

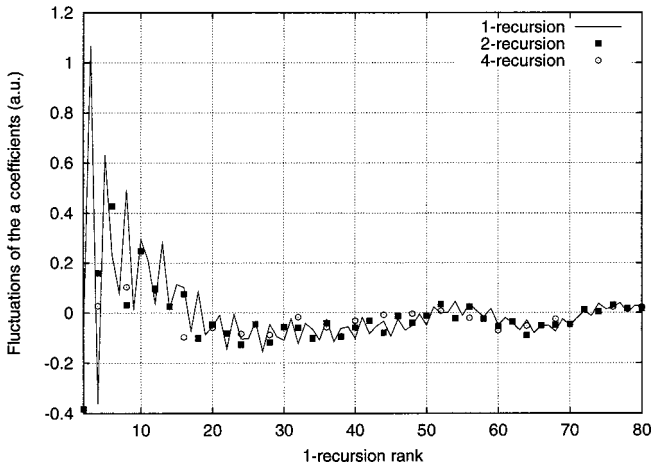

FIG. 10. Fluctuations of the recursion coefficients with steps h, $2h$, and $4h$: δa_{4N}, δA_{2N}, and $\delta \mathcal{A}_{\mathcal{N}}$. They are small and approximately superimposable when N is large. These fluctuations arise from both the kinetic and potential terms.

For the same system, we now consider two different grids, one with a spacing h, denoted the 1-grid, and the other with a spacing $2h$, denoted the 2-grid. Each cell in the 2-grid contains eight 1-grid cells. If h is small, a property calculated in a 2-grid cell is approximately an average over these eight 1-grid cells. We can iterate the procedure and define a 2^p-grid with a spacing $2^p h$. For example, each cell in the 4-grid contains eight 2-grid cells and 64 cells in the finer grid.

A recursion performed on the 2^p-grid is denoted a 2^p-recursion. The chain states it generates have the same spherical structure obtained in the 1-grid. The nth chain state, however, would roughly correspond to the $2n$th chain state calculated on the 2^{p-1}-grid and initiated from any of the eight cells included in the initial state. Indeed, Gebauer [29] has observed a strong correlation between the fluctuations of the recursion coefficients on the 2-grid ($\delta A_n, \delta B_n$) and those on the finer one ($\delta a_{2n}, \delta b_{2n}$) (Fig. 10). As proposed in [29], an explicit understanding of this property is obtained from an analysis of the LDOS.

When performing a recursion for a free electron (potential set equal to zero), fluctuations in the recursion coefficients $\delta a_n^{\text{free}}=a_n^{\text{free}}-a$ and $\delta b_n^{\text{free}}=b_n^{\text{free}}-b$ transform the constant chain LDOS (Fig. 2) into the LDOS associated with the discretized Hamiltonian (Fig. 5). Because these fluctuations are small, this modification to the LDOS can be obtained within linear response [Eq. (12)]. When performing the recursion with a step $2h$, the discretized free electron Hamiltonian is divided by a factor 4. This implies that the recursion coefficients, the bandwidth, and the zone where the $\sqrt{E}$ LDOS is correctly described are divided by this factor 4: $a=4A$, for example. The normalization introduced in Eq. (11) makes the small energy part of the free electron LDOS invariant in this change of scale.

In the general case, the LDOS accounts for the existence of a potential. The recursion coefficients have additional fluctuations: $\delta a_n^{\text{pot}}=a_n-\delta a_n^{\text{free}}-a$ and $\delta b_n^{\text{pot}}=b_n-\delta b_n^{\text{free}}-b$. These fluctuations are smaller than those shown in Fig. 10, and they vary continuously from one point to another and from one rank to another. Our objective is now to use the invariance of the LDOS in a change of grid to interpolate the

TABLE III. Correspondence of ranks from one scale to another. The associated density corrections are identical in the limit of small energies.

	4-recursion	2-recursion	1-recursion
Coefficient		N	$2N+1$
a	$\mathcal{N}$	$2\mathcal{N}+1$	$4\mathcal{N}+3$
Coefficient		N	$2N+1/2$
b	$\mathcal{N}$	$2\mathcal{N}+1/2$	$4\mathcal{N}+3/2$

$\delta a_n^{\rm pot}$ and $\delta b_n^{\rm pot}$ fluctuations on a 1-grid from the fluctuations $\delta A_n^{\rm pot}$ and $\delta B_n^{\rm pot}$ on a 2-grid. Because the additional fluctuations $\delta A_n^{\rm pot}$ and $\delta B_n^{\rm pot}$ are small, their contribution to the LDOS can also be obtained within linear response theory around the constant chain model. We now make use of this property to establish a relation between fluctuations related to different grid sizes. Since $a=2b$, $A=2B$ (see Sec. II), $a=4A$ and identifying the related corrections to the LDOS in the limit of small energies, we write

$$\sum_p \frac{\delta a_p^{\rm pot}}{\pi^2 b^{1/2}} \sin\left[(2p+2)\cos^{-1}\left(\frac{E}{2b}-1\right)\right] \approx \sum_q \frac{\delta A_q^{\rm pot}}{\pi^2 B^{1/2}} \sin\left[(2q+2)\cos^{-1}\left(\frac{E}{2B}-1\right)\right]. \quad (19)$$

Focusing on the small energies, and expanding the $\cos^{-1}$ term as $\sqrt{E/b}$ when E/b is small, the two series coincide for $\delta a_{2q+1}^{\rm pot}=2\,\delta A_q^{\rm pot}$ and $\delta a_{2q}^{\rm pot}=0$.

Since the 1-recursion coefficients contain more information than the 2-recursion ones, there is a certain freedom of choice for the interpolation formula. Because the calculated $\delta a_p^{\rm pot}$ are continuous from one rank to another, we interpolate the $\delta a_p^{\rm pot}$ for the even values of p:

$$\delta a_{2q+1}^{\rm pot}=\delta A_q^{\rm pot}, \quad (20)$$

$$\delta a_{2q}^{\rm pot}=\delta A_{q-1/2}^{\rm pot} \text{ interpolated.} \quad (21)$$

A similar identification can be performed for 4-recursions and for coefficients b. A noninteger rank is found in the latter case. This means that 1-recursion coefficients interpolate those related to a double step. The results are summarized in Table III. This interpolation scheme is still compatible with Eq. (19). An example of the correspondence between density corrections is shown in Fig. 11.

We may now compare efficiently the recursion coefficients related to different scales. Given a series a_n of recursion coefficients, we first subtract the associated free electron coefficients $a_n^{\rm free}=a+\delta a_n^{\rm free}$, so as to remove the fluctuations associated with the kinetic term. The remainder $\delta a_n^{\rm pot}=a_n-a_n^{\rm free}$ is then due to the potential. The fluctuations $\delta a_{4\mathcal{N}+3}^{\rm pot}$, $\delta A_{2\mathcal{N}+1}^{\rm pot}$, and $\delta A_{\mathcal{N}}^{\rm pot}$ are compared in Fig. 12. As expected, the fluctuations are smaller and the agreement between different scales is improved over those in Fig. 10. This scale invariance property is the basis of the multiscale approach that we now propose.

It may be remarked that this scale invariance property does not correspond to the renormalization method proposed by Giannozzi *et al.* [24]. The latter method consists of building new recursion coefficients by merging recursion steps by groups of two. The number of coefficients in the new chain is half that in the original one, as is the case with a 2-recursion. The renormalized chain, however, retains more information in the 1-recursion than can be found in the 2-recursion.

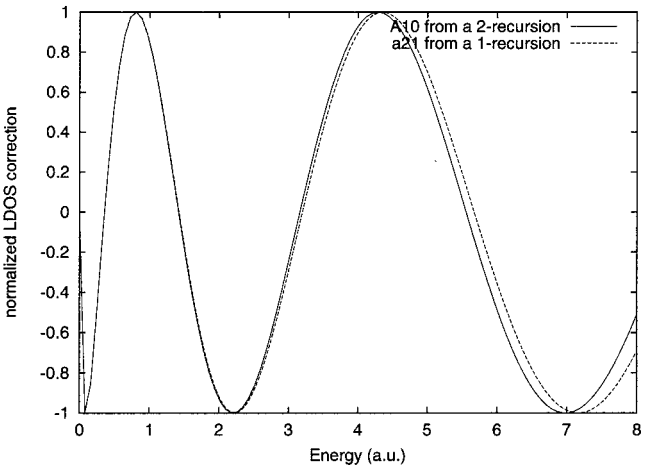

FIG. 11. Example of correspondence between density corrections to the constant chain model related to steps, h, $2h$, and $4h$. The corrections related to $a_{4\mathcal{N}+3}$, $\mathcal{A}_{2\mathcal{N}+1}$, and $\mathcal{A}_{\mathcal{N}}$ are identical in the limit of small energies.

Nevertheless, our approach allows us to interpolate distant 1-recursion coefficients from 2- and 4-recursions. We perform three recursions of 20 steps each, with grid spacings h, $2h$, and $4h$. We then constitute an interpolated chain a_n, b_n as follows. For $n\leqslant 20$, we retain the single step coefficients. For $21\leqslant n\leqslant 40$, we interpolate the potential-related fluctuations of the double step coefficients and add the free electron single step coefficient:

$$a_{2N}=a_{2N}^{\rm free}+\delta A_{\mathcal{N}-1/2}^{\rm pot}, \quad b_{2N}=b_{2N}^{\rm free}+\delta B_{\mathcal{N}-1/4}^{\rm pot},$$
$$a_{2N+1}=a_{2N+1}^{\rm free}+\delta A_{\mathcal{N}}^{\rm pot}, \quad b_{2N+1}=b_{2N+1}^{\rm free}+\delta B_{\mathcal{N}+1/4}^{\rm pot}. \quad (22)$$

Here, fractional indices indicate interpolation. For $41\leqslant n\leqslant 80$, we interpolate the quadruple step coefficients:

$$a_{4\mathcal{N}}=a_{4\mathcal{N}}^{\rm free}+\delta \mathcal{A}_{\mathcal{N}-3/4}^{\rm pot}, \quad b_{4\mathcal{N}}=b_{4\mathcal{N}}^{\rm free}+\delta \mathcal{B}_{\mathcal{N}-3/8}^{\rm pot},$$
$$a_{4\mathcal{N}+1}=a_{4\mathcal{N}+1}^{\rm free}+\delta \mathcal{A}_{\mathcal{N}-1/2}^{\rm pot}, \quad b_{4\mathcal{N}+1}=b_{4\mathcal{N}+1}^{\rm free}+\delta \mathcal{B}_{\mathcal{N}-1/8}^{\rm pot},$$
$$a_{4\mathcal{N}+2}=a_{4\mathcal{N}+2}^{\rm free}+\delta \mathcal{A}_{\mathcal{N}-1/4}^{\rm pot}, \quad b_{4\mathcal{N}+2}=b_{4\mathcal{N}+2}^{\rm free}+\delta \mathcal{B}_{\mathcal{N}+1/8}^{\rm pot}, \quad (23)$$
$$a_{4\mathcal{N}+3}=a_{4\mathcal{N}+3}^{\rm free}+\delta \mathcal{A}_{\mathcal{N}-1/2}^{\rm pot}, \quad b_{4\mathcal{N}+3}=b_{4\mathcal{N}+3}^{\rm free}+\delta \mathcal{B}_{\mathcal{N}+3/8}^{\rm pot},$$

For $n\geqslant 81$, we use the constant chain terminator with constants equal to a_{80} and b_{80}.

The computation cost grows like the fourth power of the chain length. Furthermore, the relative locations of the 4, 2, and 1-grids are such that only one 4-recursion is necessary for 64 points on the 1 grid (one 2-recursion for 8 points on the 1-grid). The multiscale strategy is therefore 224 times faster than a method in which a recursion of 80 steps would

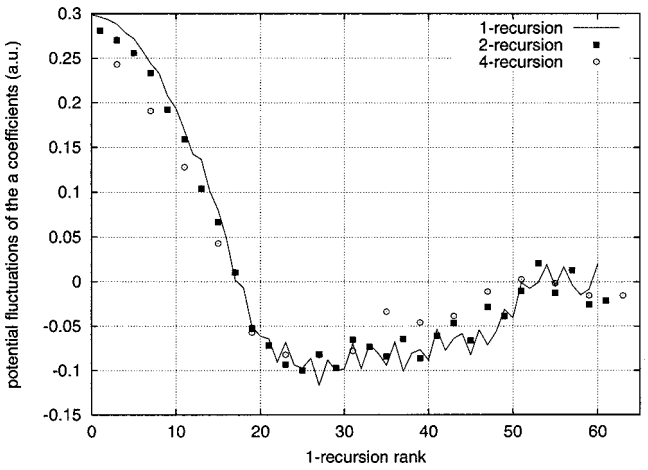

FIG. 12. Additional fluctuations of the recursion coefficients with steps h, $2h$, and $4h$: $\delta a_n^{\mathrm{pot}}$, $\delta A_{\mathcal{N}}^{\mathrm{pot}}$, and $\delta \mathcal{A}_{\mathcal{N}}^{\mathrm{pot}}$. The agreement is improved over that in Fig. 10. The fluctuations related to the kinetic term have been subtracted and a shift has been taken into account.

need to be performed in every point of the 1-grid. Let us now check the accuracy of this approximation. Figure 13 shows an example of the relative differences between the exact and interpolated recursion coefficients. The relative differences are of the order of 10^{-4} for coefficients originating from the 2-recursion, and of the order of 10^{-3} for those calculated from the 4-recursion.

These differences can be assessed in the light of the partial derivatives $\partial\rho/\partial a_n$. The derivatives are shown in Fig. 14 for a representative point in our reference system (variations of the derivatives were found to be small throughout the system). The fluctuations seen on the figure are related to Friedel's oscillations. The fluctuations tend to zero and this means that the remote details of the potential will have a limited impact on the density where the recursion was initiated. Given our choice of discretization, the density is most sensitive to the coefficients with ranks smaller than 20. We therefore retain exact coefficients up to this rank. The smaller amplitudes of the derivatives with higher ranks justify the use of an approximation for the corresponding coefficients

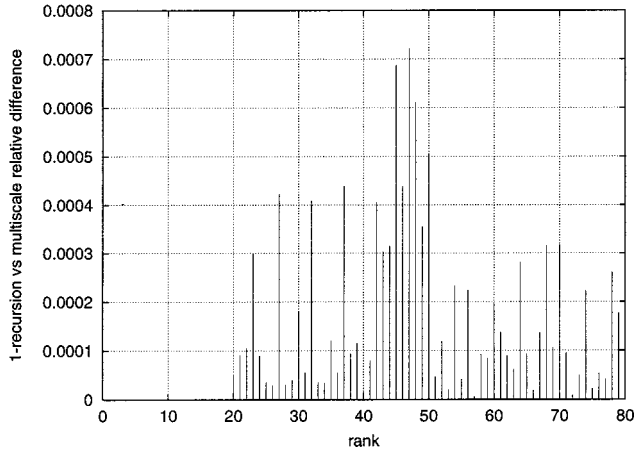

FIG. 13. Relative differences between the a_n calculated in a recursion of 80 steps and the coefficients deduced from our interpolation procedure.

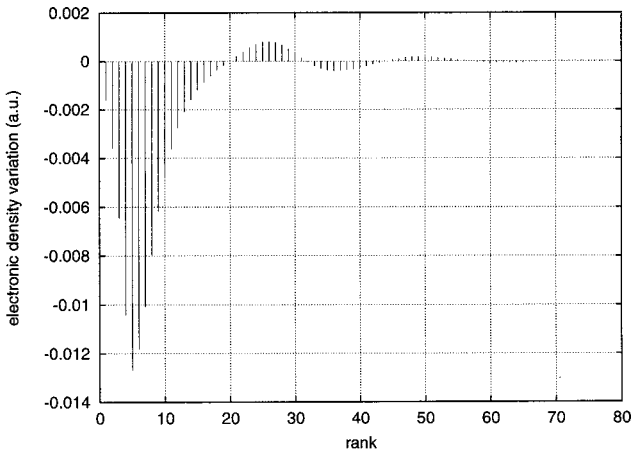

FIG. 14. Values of $\partial\rho/\partial a_n$ calculated for a representative point in our model system.

(interpolation or constant chain value).

We finally compare the density ρ_R calculated in the reference system with our method, and the density ρ_A calculated with the FEMD code. Our recursion calculation is performed in an extended cell, meaning that the chain states extend into the images of the simulation cell. Our result is therefore compared with the reference FEMD calculation performed with eight k points. The results are shown in Fig. 15. The observed differences are smaller than 2%. This accuracy validates our multiscale approach. We now turn to the computation time required by the method.

VI. DISCUSSION

A direct comparison of computation time with the FEMD code is not so easy. During the self-consistent calculation, it took an average of 1 min 40 sec for FEMD to calculate the electronic density from the electronic potential on 64 processors of the T3E Cray computer of Bruyères-le-Châtel. This computation time is the best we obtained using this machine. The computation time using 128 processors is considerably larger than that with 64 processors, since the communication time increases with the number of processors. Our multiscale recursion took 9 min 30 sec to calculate the density using 128 processors. Although this computation time is larger, the

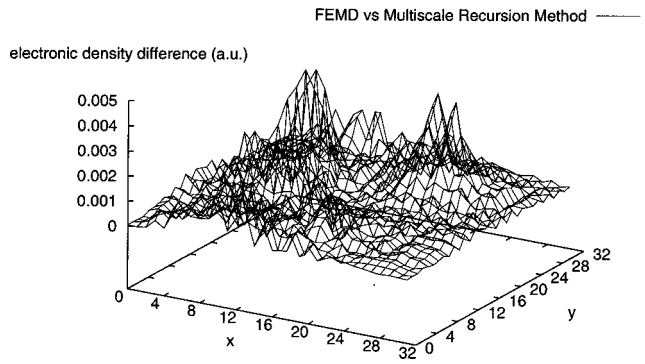

FIG. 15. $|\rho_R - \rho_A|$: Map of differences between the FEMD density using eight k points, and the multiscale recursion performed in an extended cell.

scaling properties of our method make this a very good result.

Because recursion calculations are independent from one point to another, the computation cost is proportional to the size of the system. Our method is competitive with FEMD when the size of the system is increased. A system of 96 hydrogen atoms would require six times as much time with our method, and $6^2=36$ times as much with FEMD. Both methods would need the same time on the T3E Cray in this case, but the balance falls in favor of the recursions for larger systems.

The recursions, however, can be distributed on an arbitrary number of processors. When running the program on a parallel computer (or on a farm of workstations), it suffices to distribute grid points into small groups which are then dispatched to processors. In our multiscale approach, the groups retained are the 4-grid cells, which are groups of 64 cells in the 1-grid. The recursion calculations can then be performed without communication between processors, and the total computation time is simply divided by the number of processors used. The use of massively parallel computing would definitely make the recursion method faster.

Another important property of the recursion is its behavior with respect to temperature. Unlike schemes in which eigenstates are computed (FEMD, for example), the calculation of the density in the recursion framework is faster at higher temperature. The 3 eV temperature that we considered is the highest limit that can reasonably be simulated with FEMD. By contrast, this temperature is low for the recursion scheme to be efficient. Shorter chains are sufficient at higher temperatures. As an example, we find that series of 40 recursion coefficients are sufficient to converge the density if we assume a temperature of 10 eV (calculation performed with the model potential used at 3 eV). A multiscale strategy involving 10 recursions on 1, 2, and 4-grids then requires about 40 sec to calculate the electronic density on 128 processors.

Our reference system permits an accurate comparison with FEMD calculations. But it was not designed to highlight the advantages of the recursion method. It is too small, and the temperature is low. Although it was imagined eight years ago, the recursion method in real space has never been used to our knowledge, because of a prohibitive computation time. The multiscale approach that we have constructed and implemented cuts down this computation time by two orders of magnitude, thus opening a different approach to the *ab initio* simulation of hydrogen plasmas. The computation time is now of the order of magnitude of that of the reference method, and could become smaller by means of massively parallel computing. Future work includes (1) reaching self-consistency and (2) implementing the scheme within a molecular dynamics code. Regarding the first point, an attractive strategy would consist of performing scalewise self-consistent calculations.

ACKNOWLEDGMENTS

We wish to thank Thierry Deutsch for his help with FEMD code and *k* points, and Ralph Gebauer who sent us a copy of his master's thesis. We also thank Patrick Blottiau, Jean Clérouin, and Pierre Noiret for useful discussions.

[1] D. J. Stevenson, J. Phys.: Condens. Matter **10**, 11 227 (1998).
[2] S. T. Weir, J. Phys.: Condens. Matter **10**, 11 147 (1998).
[3] D. Saumon and G. Chabrier, Phys. Rev. Lett. **66**, 64 (1989).
[4] J. Clérouin and S. Bernard, Phys. Rev. E **56**, 3534 (1997).
[5] C. Pierleoni, D. M. Ceperley, B. Bernu, and W. R. Magro, Phys. Rev. Lett. **73**, 2145 (1994).
[6] I. Kwon, L. A. Collins, J. D. Kress, N. Trouiller, and D. L. Lynch, Phys. Rev. E **49**, 4771 (1994).
[7] J. Clérouin, E. L. Pollock, and G. Zérah, Phys. Rev. A **46**, 5130 (1992).
[8] G. Zérah, J. Clérouin, and E. L. Pollock, Phys. Rev. Lett. **69**, 446 (1992).
[9] A. Alavi and D. Frenkel, J. Chem. Phys. **97**, 9249 (1992).
[10] A. Alavi, J. Kohanoff, M. Parrinello, and D. Frenkel, Phys. Rev. Lett. **73**, 2599 (1994).
[11] A. Alavi, M. Parrinello, and D. Frenkel, Science **269**, 1252 (1995).
[12] A. Alavi, *Monte Carlo and Molecular Dynamics of Condensed Matter Systems* (Italian Physical Society, Bologna, 1995), pp. 649–66.
[13] A. Alavi, Curr. Opin. Solid State Mater. Sci. **1**, 846 (1996).
[14] A. Alavi, P. Hu, T. Deutsch, P. L. Sivestrelli, and J. Hutter, Phys. Rev. Lett. **16**, 3650 (1998).
[15] F. Gygi, Phys. Rev. B **48**, 11 692 (1993).
[16] S. Baroni and P. Giannozzi, Europhys. Lett. **17**, 547 (1992).
[17] S. Goedecker and L. Colombo, Phys. Rev. Lett. **73**, 122 (1994).
[18] A. P. Horsfield, A. M. Bratkovsky, M. Fearn, D. G. Pettifor, and M. Aoki, Phys. Rev. B **53**, 12 694 (1996).
[19] S. Goedecker, Phys. Rev. B **58**, 3501 (1998).
[20] N. D. Mermin, Phys. Rev. **137**, 1441 (1965).
[21] R. G. Parr and W. Yang, *Density-Functional Theory of Atoms and Molecules* (Oxford Science, New York, 1989).
[22] R. Haydock, J. Phys. A **7**, 2120 (1974).
[23] R. Haydock, Solid State Phys. **35**, 215 (1980).
[24] P. Giannozzi, G. Grosso, S. Moroni, and G. Pastori Parravicini, Appl. Numer. Math. **4**, 273 (1988).
[25] C. Lanczos, J. Res. Natl. Bur. Stand. **45**, 255 (1950).
[26] A. Baldereschi, Phys. Rev. B **7**, 5212 (1973).
[27] D. J. Chadi and M. L. Cohen, Phys. Rev. B **8**, 5747 (1973).
[28] H. J. Monkhorst and J. D. Pack, Phys. Rev. B **13**, 5188 (1974).
[29] R. Gebauer, Master thesis, CECAM, 1997 (unpublished).